

Structures and Properties of *trans*-1,3,3,3-Tetrafluoropropene (HFO-1234ze) and 2,3,3,3-Tetrafluoropropene (HFO-1234yf) Refrigerants

Jan Schwabedissen,^[a] Timo Glodde,^[a] Yury V. Vishnevskiy,^[a] Hans-Georg Stammer,^[a] Lukas Flierl,^[b] Andreas J. Kornath,^{*[b]} and Norbert W. Mitzel^{*[a]}

The refrigerant *trans*-1,3,3,3-tetrafluoropropene (HFO-1234ze) is used as a replacement for former cooling agents that have been phased-out due to their global warming potential or ozone depleting potential. Although it is used on a large scale, only a few vibrational data and no structural data of HFO-1234ze are known. We report structure determinations based on low-temperature single-crystal X-ray diffraction data as well

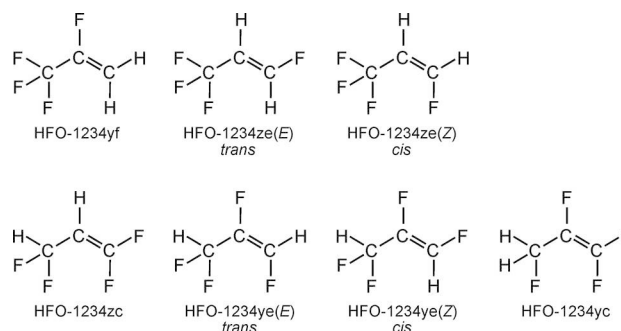
as gas-phase diffraction data of HFO-1234ze and HFO-1234yf (2,3,3,3-tetrafluoropropene). Furthermore, vibrational spectra of HFO-1234ze in all phases are described. The results are discussed together with quantum-chemical calculations on the PBE0/cc-pVTZ level of theory. Combustion experiments of HFO-1234ze show carbonyl difluoride, carbon dioxide and hydrogen fluoride to be the main combustion products.

1. Introduction

Hydrofluoroolefines (HFO) are discussed as environmentally more friendly replacements^[1] of common refrigerants like hydrofluorocarbons (HFC) as they have zero ODP (ozone depletion potential) and low GWP (global warming potential).^[2] Among the tetrafluoropropenes shown in Scheme 1 the isomers HFO-1234yf and HFO-1234ze(*E*) are used as refrigerants.

Many previous investigations aim to reveal information about thermodynamic properties^[3] or structural behavior in the liquid phase^[4] or even as building blocks in polymers.^[5] Hitherto only HFO-1234yf (2,3,3,3-tetrafluoropropene) was structurally characterized in the gas phase by microwave spectroscopy^[6] and in the solid state by single crystal X-ray diffraction,^[7] but no elucidation of the structural behavior of the isomer HFO-1234ze(*E*) (*trans*-1,3,3,3-tetrafluoropropene) has been reported yet.

Herein we report about the molecular structures of *trans*-1,3,3,3-tetrafluoropropene (*trans*-1333TFP, **1**) and 2,3,3,3-tetrafluoropropene (2333TFP, **2**) in the vapor phase by gas-



Scheme 1. Isomers of tetrafluoropropene (commercial abbreviations).

phase electron diffraction (GED) and in the solid state by high angle X-ray diffraction along with the electron density distributions of both substances. Furthermore, the vibrational spectra and combustion properties for **1** are described.

2. Results and Discussion

2.1. Calculations

For the determination of possible conformers of 1,3,3,3-tetrafluoropropene (**1**) and 2,3,3,3-tetrafluoropropene (**2**), the potential energy curves at the PBE0^[8]/cc-pVTZ^[9] level of theory were calculated for the rotation of the trifluoromethyl group about the C–C bond (Figure 1). As for **1** *trans* and *cis* isomers exist, both were studied regarding the barrier for the rotation of the CF₃ group.

In Figure 1 all three graphs show a minimum at a dihedral angle φ (FCCX) of 60° and 180° due to local C_{3v} symmetry of the CF₃ group. In all three cases, this is a conformation of C_s symmetry with the trifluoromethyl group being staggered regarding the substituent at the adjacent carbon atom, fluorine

[a] Dr. J. Schwabedissen, T. Glodde, Dr. Y. V. Vishnevskiy, Dr. H.-G. Stammer, Prof. Dr. N. W. Mitzel
Lehrstuhl für Anorganische Chemie und Strukturchemie
Fakultät für Chemie Universität Bielefeld
Universitätsstraße 25
33615 Bielefeld (Germany)
E-mail: mitzel@uni-bielefeld.de

[b] L. Flierl, Prof. Dr. A. J. Kornath
Department of Chemistry
Ludwig-Maximilian University
Butenandtstraße 5–13 (Haus D)
81377 Munich (Germany)
E-mail: Andreas.kornath@cup.uni-muenchen.de

Supporting information for this article is available on the WWW under <https://doi.org/10.1002/open.202000172>

© 2020 The Authors. Published by Wiley-VCH GmbH. This is an open access article under the terms of the Creative Commons Attribution Non-Commercial NoDerivs License, which permits use and distribution in any medium, provided the original work is properly cited, the use is non-commercial and no modifications or adaptations are made.

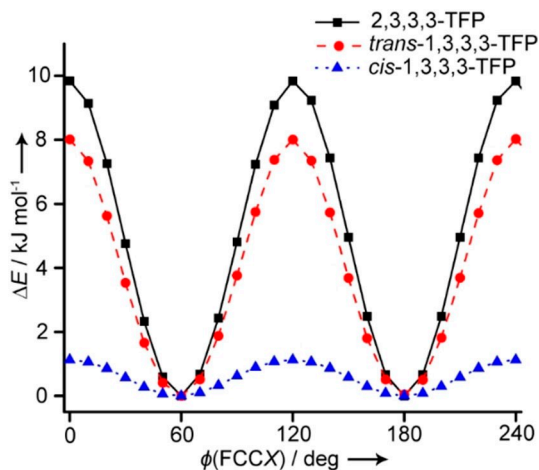


Figure 1. Scan of the potential energy for the rotation of the trifluoromethyl group around the C–C single bond for the three different isomers of tetrafluoropropene. X=H for both 1,3,3,3-tetrafluoropropenes and X=F for 2.

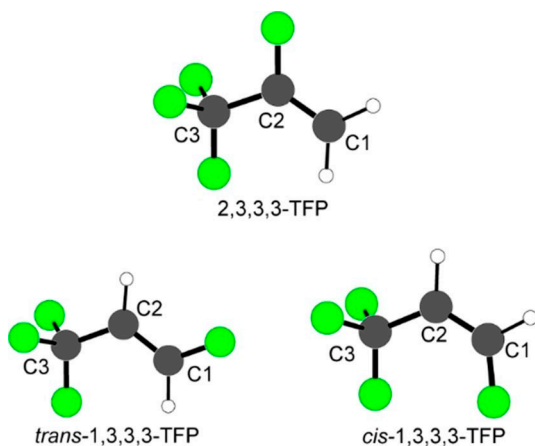


Figure 2. Optimized minimum structures of the conformers of three isomers of tetrafluoropropene.

for 2 and hydrogen for 1. The barriers of rotation found at 120° are 10 kJ mol⁻¹ for 2 and 8 kJ mol⁻¹ for *trans*-1. At this point, about 2 kJ mol⁻¹ more energy is required for the rotation of the trifluoromethyl group in 2, because the fluorine atom is sterically more demanding than the hydrogen atom. However, the energy profile of *cis*-1 differs from the two mentioned above in a manner that a relatively low barrier for the rotation of about 1 kJ mol⁻¹ can be found. The reason for this low barrier is steric repulsion occurring in the minimum structure between the CF₃ group and the fluorine atom at C1, which can be considered as a manifestation of 1,3-interactions. The local maximum is found, as for all three isomers of tetrafluoropropene, for an eclipsed conformation of the CF₃ group regarding the substituent at C2. In Figure 2 all three minimum structures are depicted.

The double bond between C1 and C2 as well as the bond to the fluorine atom from a planar coordinated carbon atom are not much affected by the variation of the position of the fluorine atom. In contrast, the carbon–carbon single bond is

significantly longer when a fluorine atom is attached to C2, which confirms the higher steric demand of fluorine compared to hydrogen. The largest angle at the carbon scaffold is found for the staggered conformer of the *cis*-isomer of 1, which might be due to the steric interaction of the trifluoromethyl group with the fluorine atom at carbon C1.

2.2. Crystal Structures

For the determination of the molecular structures of *trans*-1 and 2 in the solid state, a small amount of each substance was condensed into a capillary, which was flame sealed. Suitable crystals^[10] were grown from the liquid by the *in situ* crystallization technique by manually generating a crystal seed at a temperature just below the melting point and subsequent cooling. For details of the procedure as well as crystallographic details, see the Supporting Information (Table S2). For both crystals high-angle scattering data were recorded to determine their charge density topologies.

Molecular structures in the solid state are depicted in Figure 3 and selected structural parameters of 1 and 2 are listed in Table 1. In the solid state, 1 resides on a crystallographic mirror plane, accordingly with a dihedral angle $\varphi(\text{H2–C2–C3–F2})$ of 180°. However, 2 shows only approximately molecular C_s symmetry with the corresponding dihedral angle $\varphi(\text{F1–C2–C3–F4})$ measuring 178.7(1)°. In line with the computationally determined structures, the distance C1–C2 is affected only slightly by the position of the fluorine atom (1.318(1) Å resp. 1.313(1) Å). Anyhow, the bond C2–C3 to the CF₃ group is almost 0.02 Å longer in 2 than the corresponding bond in 1 (1.496(1) resp. 1.479(1) Å). In addition to the fact that the fluorine atom is sterically more demanding than the hydrogen atom, its high electronegativity induces a higher positive charge at the carbon atom. The charge can be obtained from the experimentally determined electron density distribution. Hence, in 1 the charge of C2 amounts to +0.07 e and for C3 +1.93 e whereas in 2 the charges are even larger at +0.60 e and +2.05 e for C2 and C3, respectively. Both properties lead to a longer C2–C3 bond in 2 compared to that in 1. Concerning the trifluoromethyl group, the C–F bond eclipsing the C–C double bond, is in both structures shorter by 0.01 Å than that to the two out-of-plane fluorine atoms. The same structural feature is observed in the solid state structure of hexafluoropropene.^[11] The $\angle(\text{H1–C1–X})$ angle in the case of X=F for 1 (114.0(4)°) is about 9° smaller than in 2 (123.3(5)°) where X=H. Furthermore,

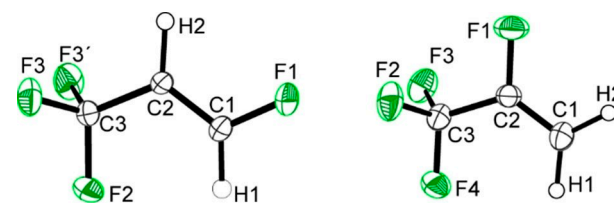


Figure 3. Molecular structures in the solid state of *trans*-1 (left) and 2 (right) (50% probability displacement ellipsoids). Symmetry code: $(-\frac{1}{2}+x, \frac{1}{2}-y, \frac{1}{2}-z)$.

Table 1. Structural parameters in the solid state (XRD) and in the gas phase (GED, r_e) of 1,3,3,3-tetrafluoropropene and 2,3,3,3-tetrafluoropropene. Distances r are given in Å and angles \angle in degrees. Errors in XRD are given as three times standard deviations (3σ) and total errors (from the Monte-Carlo method) are reported for the gas-phase structures.

Parameter ^[a]	1 (XRD) r_α	1 (GED) r_e	2 (XRD) r_α	2 (GED _{comb}) r_e
$r(\text{C1}-\text{C2})$	1.3181(3)	1.321(4)	1.3134(4)	1.323(8)
$r(\text{C2}-\text{C3})$	1.4789(3)	1.481(6)	1.4963(4)	1.498(4)
$r(\text{C1}-\text{H1})$	1.054(17)	1.101(9)	1.071(4)	1.083(13)
$r(\text{C1}-\text{X})$	1.3407(5)	1.326(4)	1.075(3)	1.085(13)
$r(\text{C2}-\text{Y})$	1.084(14)	1.101(9)	1.3373(5)	1.333(3)
$r(\text{C3}-\text{F2}/4)^c$	1.3350(5)	1.336(4)	1.3302(6)	1.331(3)
$r(\text{C3}-\text{F3}/2)^c$	1.3468(5)	1.337(4)	1.3412(6)	1.334(3)
$r(\text{C3}-\text{F3}'/3)^c$	1.3468(5)	1.337(4)	1.3422(6)	1.334(3)
$\angle(\text{C1}-\text{C2}-\text{C3})$	121.53(2)	120.8(8)	126.69(3)	125.8(2)
$\angle(\text{H1}-\text{C1}-\text{X})$	114.0(4)	116.0(15)	123.3(5)	120.4 ^[b]
$\angle(\text{C1}-\text{C2}-\text{Y})$	121.8(4)	121.6 ^[b]	122.59(4)	122.8(4)
$\angle(\text{C3}-\text{C2}-\text{Y})$	116.7(4)	117.6(8)	110.73(4)	111.4(4)
$\angle(\text{F2}-\text{C3}-\text{C2})^d$	106.98(3)	113.0(5)	111.66(3)	111.3(4)
$\angle(\text{F3}-\text{C3}-\text{C2})^d$	111.81(2)	111.7(5)	111.63(4)	111.0(4)
$\angle(\text{F4}-\text{C3}-\text{C2})^d$	111.81(2)	111.7(5)	111.40(4)	111.0(4)
$\angle(\text{F3}-\text{C3}-\text{F4})^d$	105.63(5)	106.3(5)	107.19(5)	107.3(7)

[a] X=F for 1 and X=H for 2, Y=H for 1 and Y=F for 2, [b] Parameter fixed at the computational value. [c] Numbering for 2. [d] Analogous parameters for 2 are given.

in hexafluoropropene the angle F–C1–F measures 111.9(3)°. This is in good agreement with the explanation that fluorine atoms generally prefer orbitals of their binding partners with small s and thus higher p character, when forming covalent polar bonds.^[12] In comparison, the double bond in the perfluorinated propene is slightly shorter at 1.307(5) Å due to the higher degree of fluorination, whereas the length of the carbon–carbon single bond in hexafluoropropene (1.486(5) Å) falls between the corresponding ones in 1 and 2. A systematic study on solid-state structures of fluorinated ethenes has been performed to investigate the structural effects on the double bond, but revealed no systematic behavior of increase or decrease of the bond length of the double bond upon fluorination of the C=C backbone.^[13]

Aggregation of single molecules in the solid state occurs mainly through F...H contacts like it was previously examined for partially fluorinated olefins 1,1,4,4-tetrafluorobutadiene,^[14] 1,1,2-trifluorobuta-1,3-diene^[15] as well as for a series of fluorinated ethenes.^[13] In the crystal structure of 1 the shortest H...F contacts can be found within the crystallographic mirror plane with 2.44(1) Å and 2.63(1) Å length (Figure 4). Both contacts are less than the sum of the corresponding van der Waals radii (2.66 Å).^[16] Because the ethylene units are facing each other, a planar double strand polymer is build up. These strands are linked with H...F contacts of 2.72(1) Å length within the mirror plane from the H2 atom to the symmetric equivalent fluorine atoms. These planes are linked with H...F contacts of 2.83(1) Å. In the related ethene (*E*)-1,2-difluoroethene molecules are connected by H...F contacts of 2.59 Å length.

Similar to the extended solid-state structure of (*E*)-1,2-difluoroethene, the extended structure of 1 in the crystalline phase shows parallel layers of molecules (Supporting Informa-

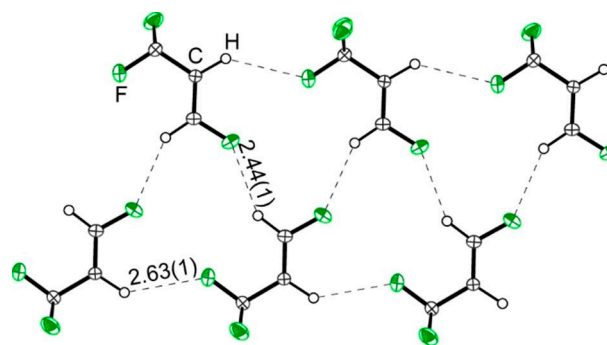


Figure 4. Aggregation in the solid-state structure of *trans*-1,3,3,3-tetrafluoropropene.

tion, Figure S11). The distance between the planes is half of the crystallographic b axis (3.28 Å).

The crystal structure of 2 contains dimers formed by H...F contacts of 2.60(1) Å length. These dimers are linked to each other by H...F contacts of 2.59(1) Å length (Figure 5). The central H1-F4-H1'-F4' planes of the different dimers are tilted by 24.6(3)°. In the analogous ethene, 1,1-difluoroethene, columns are formed with the positively charged hydrogen atoms pointing at the negatively charged fluorine atoms, but no short H...F contacts are reported.

The extended solid-state structure shows a herringbone like arrangement of the molecules along the c -axis (Supporting Information, Figure S12). A similar pattern was also observed for 1,1,4,4-tetrafluorobutadiene.^[14]

2.3. Charge Density and Topological Analysis

On the basis of high-resolution X-ray diffraction at low temperature, the charge density $\rho(r)$ was determined^[17] for both crystal structures mentioned above. Along with the experimental deduced densities the theoretical ones, from MP2(full)/aug-cc-pVTZ calculation^[13] and evaluated with the AIMALL program,^[18]

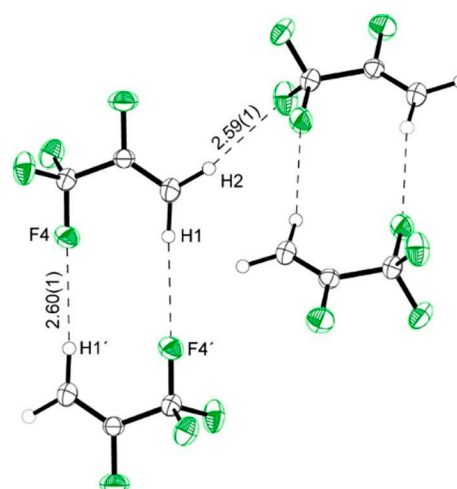


Figure 5. Aggregation of 2,3,3,3-tetrafluoropropene in the crystal phase.

Table 2. Values taken from the experimental electron density for both molecules in the crystal phase in comparison with computed values at the MP2(full)/aug-cc-pVTZ level (experiment/theory). Electron densities at bond critical points $\rho(r_{\text{bcp}})$ are given in $e \text{ \AA}^{-3}$ the Laplacian $-\nabla^2\rho(r_{\text{bcp}})$ in $e \text{ \AA}^{-5}$ and the ellipticity ϵ is dimensionless, d_1 is defined as the distance of the first atom to the bond critical point along the bond path.

Bond ^a	Bond path length		d_1		$\rho(r_{\text{bcp}})$		$-\nabla^2\rho(r_{\text{bcp}})$		ϵ	
	1	2	1	2	1	2	1	2	1	2
C1–C2	1.3181(3)/ 1.3211	1.3134(4)/ 1.3180	0.700/ 0.728	0.638/ 0.555	2.41(1)/ 2.48	2.47(1)/ 2.47	–27.15(2)/ –31.88	–28.25(4)/ –31.23	0.33/ 0.43	0.23/ 0.39
C2–C3	1.4789(3)/ 1.4766	1.4963(4)/ 1.4946	0.638/ 0.687	0.697/ 0.719	1.95(1)/ 1.95	1.95(1)/ 1.96	–20.70(2)/ –21.78	–21.23(3)/ –21.99	0.04/ 0.05	0.04/ 0.09
C1–H1	1.054(17)/ 1.058	1.071(4)/ 1.057	0.722/ 0.716	0.760/ 0.702	1.88(1)/ 2.07	1.76(1)/ 2.00	–22.19(8)/ –31.53	–19.68(2)/ –29.13	0.11/ 0.04	0.05/ 0.01
C1–X	1.3407(5)/ 1.3311	1.075(3)/ 1.055	0.469/ 0.432	0.736/ 0.702	1.93(1)/ 1.83	1.71(1)/ 1.99	–19.08(4)/ 5.62	–17.14(2)/ –28.89	0.03/ 0.10	0.04/ 0.01
C2–Y	1.084(14)/ 1.057	1.3373(5)/ 1.3351	0.713/ 0.705	0.507/ 0.435	1.79(1)/ 1.98	2.03(1)/ 1.82	–18.54(5)/ –21.78	–23.52(8)/ 4.69	0.14/ 0.01	0.15/ 0.20
C3–F2/ C3–F4 ^b	1.3350(5)/ 1.3398	1.3302(6)/ 1.3328	0.433/ 0.441	0.424/ 0.439	2.03(1)/ 1.91	1.98(1)/ 1.94	–21.27(7)/ 5.46	–7.44(10)/ –5.01	0.05/ 0.12	0.25/ 0.12
C3–F3/ C3–F2 ^b	1.3468(5)/ 1.3421	1.3422(6)/ 1.3363	0.433/ 0.443	0.433/ 0.441	1.99(1)/ 1.91	1.93(1)/ 1.93	–18.90(6)/ –6.18	–12.07(10)/ –5.78	0.13/ 0.12	0.13/ 0.12
C3–F3 ^b		1.3421(6)/ 1.3363		0.430/ 0.441		1.89(1)/ 1.93		–9.28(10)/ –5.78		0.07/ 0.12

[a] X=F for 1 and X=H for 2, Y=H for 1 and Y=F for 2. [b] Numbering for 2,3,3,3-tetrafluoropropene 2.

were topologically characterized based on Bader's quantum theory of atoms in molecules (QTAIM).^[19] Table 2 contains the characteristic values for the electron density topology at the bond critical points [bcp, at the location r_{bcp} where $\nabla\rho(r_{\text{bcp}})=0$]. The experimental densities for both species are well reproduced by the *ab initio* method, whereas larger discrepancies in the Laplacian of the electron density $-\nabla^2\rho(r_{\text{bcp}})$ especially for the C–F bonds are observed. Particularly, the Laplacians in the bonds to the vinylic fluorine atoms feature charge depletions in the theoretical electron density (5.62 and 4.69 $e \text{ \AA}^{-5}$ for 1 and 2, respectively) whereas the experimentally determined Laplacians have large negative values of $-19.08(4)$ and $-23.52(8)$ $e \text{ \AA}^{-5}$, respectively; this indicates a strongly covalent character of the bonds. The frequently reported failure of theory to describe the electron density distribution in C–F bonds properly has also been observed in preceding studies on fluorinated olefins and aromatics.^[13,14,20] Regarding the experimental findings for the bonds to the vinylic fluorine atoms, the charge density is higher in magnitude for the fluorine atom in 2 position $\rho(r_{\text{bcp}})=2.03$ versus $1.93(1)$ $e \text{ \AA}^{-3}$ as well as the Laplacian $-\nabla^2\rho(r_{\text{bcp}})$ ($-23.52(8)$ versus $-19.08(4)$ $e \text{ \AA}^{-5}$). Along with this, the bond length is slightly shorter in the 2 isomer (1.3373(5) versus 1.3407(5) \AA).

These findings might indicate a conjugative effect with the double bond also manifest in the depicted charge density (Figure 6) where electron densities higher than 2.0 $e \text{ \AA}^{-3}$ are also found along the corresponding bonds. Substitution of a fluorine atom by a CF_3 group takes no significant effect on the electron densities in the double bonds. While for 1,1-difluoroethene $\rho(r_{\text{bcp}})=2.55(5)$ / $2.56(5)$ $e \text{ \AA}^{-3}$, the charge density at the critical point of the double bond in 2 is $2.47(1)$ $e \text{ \AA}^{-3}$, which is the same trend for (*E*)-difluoroethene ($2.47(3)$ $e \text{ \AA}^{-3}$) and 1 ($2.41(1)$ $e \text{ \AA}^{-3}$).

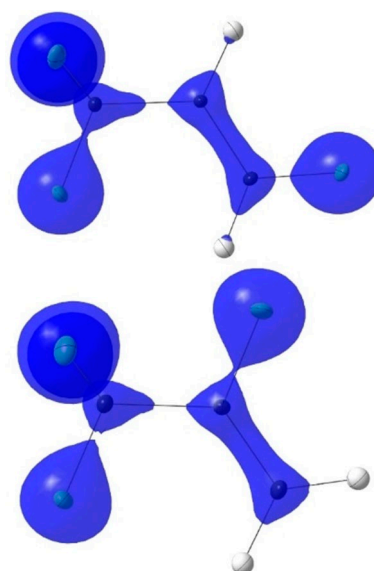


Figure 6. Isodensity surfaces ($\rho(r)=2.0$ $e \text{ \AA}^{-3}$) of the electron densities of *trans*-1 (upper) and 2 (lower).

2.4. Gas-Phase Structures

Structures of free molecules of *trans*-1 and 2 were determined by gas-phase electron diffraction (GED). For details of the experiment as well as the structural analysis, see Supporting Information. The radial distribution curves are depicted in Figure 7 and Figure 8 for *trans*-1 and 2, respectively. Structural parameters are listed in Table 1. Both refined model structures show good agreement with the experimental data with overall $R_f=3.3\%$ (1) and 2.3% (2). For the determination of total overall errors for the structural parameters, the earlier described Monte-Carlo method^[21] was applied. Microwave spectroscopy data were available for 2,^[6] and consequently its structure was refined based on the combination of electron-diffraction data

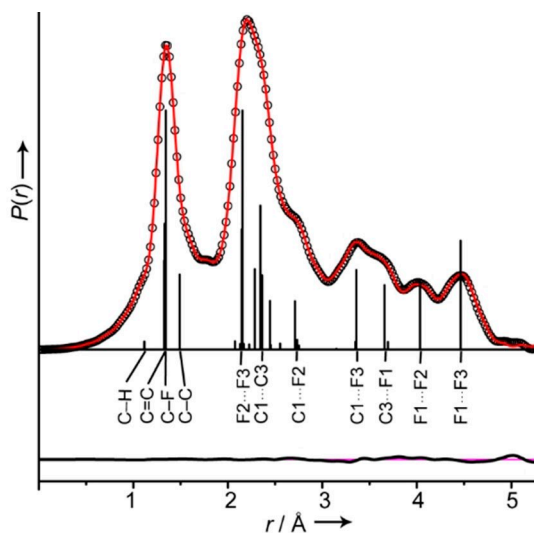


Figure 7. Experimental (O) and model (—) radial distribution curves of 1. The difference curve is below. Vertical bars indicate interatomic distances; selected ones are labelled.

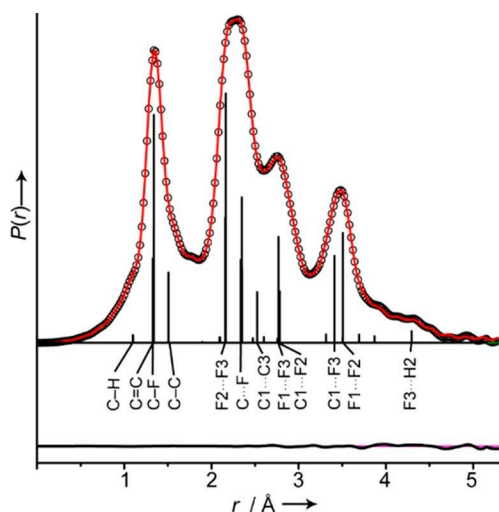


Figure 8. Experimental (O) and model (—) radial distribution curves of 2. The difference curve is below. Vertical bars indicate interatomic distances; selected ones are labelled.

and the reported rotational constants. Table 3 lists the experimental rotational constants (B_0) for different isotopologues along with the constants modelled from the structure determined by GED and the corrections ($B_e - B_0$). Corrections were taken from anharmonic frequency calculations. The small differences between the rotational constants derived from the combined microwave/electron diffraction experiment (GED_{comb}) and the ones measured by microwave spectroscopy prove the satisfying accordance of both methods.

In both cases, the structural parameters of free molecules coincide well with the respective parameters in the solid state. However, all bonds are slightly shorter in the solid state than in the gas phase and the difference between the C–F bonds in the

Table 3. Reported experimental (MW)^[6] rotational constants, calculated corrections $B_e - B_0$, B_e calculated from the commonly refined (GED_{comb}) structure and difference between refined and reported value in B_e for different isotopologues of 2.

	B_0 from MW	$B_{e(\text{calcd})} - B_0$	B_e from GED _{comb}	$\Delta(B_e)$ [MW – GED _{comb}]
CF ₃ CFCH ₂				
A_0	3714.71903(50)	18.886	3733.571	0.034
B_0	2465.51465(39)	17.878	2483.452	–0.056
C_0	2001.06445(38)	11.884	2012.860	0.118
¹³ CF ₃ CFCH ₂				
A_0	3671.50110(17)	18.549	2689.667	0.383
B_0	2431.99032(97)	17.724	2450.990	–0.276
C_0	1967.24810(93)	11.754	1978.921	0.080
CF ₃ ¹³ CFCH ₂				
A_0	3714.13390(15)	18.773	3723.895	0.012
B_0	2454.73533(91)	17.620	2472.440	–0.084
C_0	1993.82750(97)	11.697	2005.424	0.100
CF ₃ CF ¹³ CH ₂				
A_0	3714.98250(12)	18.603	3733.559	0.027
B_0	2462.24116(65)	17.631	2479.954	–0.082
C_0	1998.93819(69)	11.772	2010.558	0.102

CF₃ group vanish in the gas phase within the error ranges, because it cannot be resolved satisfactorily.

The carbon–carbon double bond in 3,3-trifluoropropene^[22] ($r_g = 1.318(8)$ Å) is shorter than that in propene ($r_g = 1.342(2)$ Å), likely due to induction of a negative charge at the carbon atom bearing the CF₃ group. Changing the CF₃ to a fluorine substituent does not have the same shortening effect on the carbon–carbon double bond in fluoroethene ($r_g(\text{C}=\text{C}) = 1.333(1)$).^[23] For the here examined species the length of the C=C bond is between those of propene and trifluoropropene, at $r_g(\text{C}=\text{C}) = 1.328(4)$ (1) and 1.330(8) Å (2). Thus, the fluorine substituents in 1 and 2 are decreasing the effect of the trifluoromethyl group regardless the position of substitution. This tendency for a shorter C=C bond upon exchange of CF₃ by fluorine was also observed for the pair *trans*-1,2-difluoroethene (1.329(4) Å)^[23] and *trans*-1,1,4,4,4-but-2-ene (1.296(20) Å).^[24] However, for 1,1-bis(trifluoromethyl)ethene (1.373(13) Å)^[25] and 1,1-difluoroethene (1.311(35),^[26] 1.316(2),^[23] 1.340(6) Å)^[27] the trend is reversed. Furthermore, the gas-phase structure of hexafluoropropene^[28] provides no hint for the systematic behavior of fluorine or CF₃ substitution on the C=C double bond. Hence, no conclusions on the systematic effects of fluorine substituents and CF₃ substituents can be drawn.

2.5. Vibrational Spectra

The gas-phase infrared spectrum and the Raman spectra of all three states of *trans*-1 are displayed in Figure 9. Additionally, Raman spectra in noble gas matrices were performed in order to obtain fundamental vibrations not affected by intermolecular interactions (see Supporting Information). Selected vibrational data together with quantum-chemically calculated frequencies at the PBE0/cc-pVTZ level of theory are listed in Table 4. The assignments were made by consideration of the Cartesian

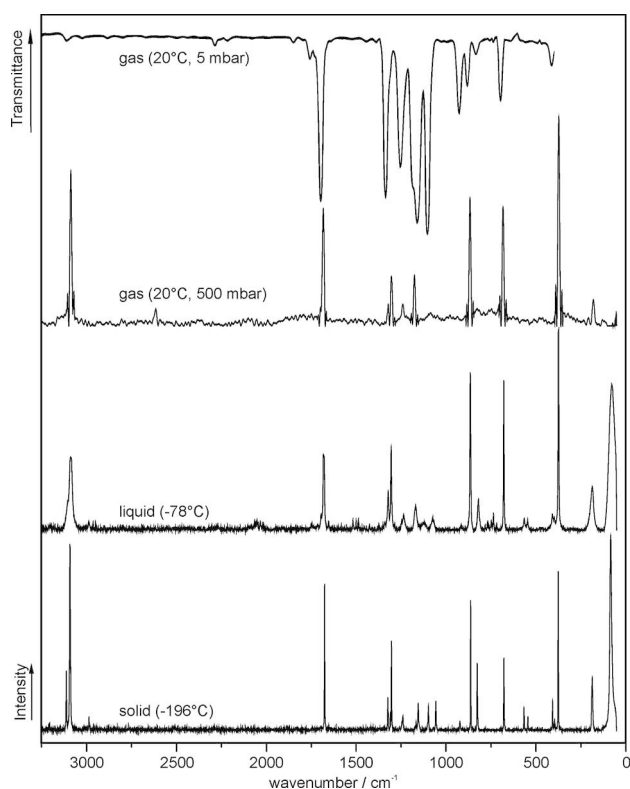


Figure 9. Infrared spectrum (gas (5 hPa), top) and Raman spectra (gas (500 hPa), liquid, solid) of **1**.

Table 4. Selected experimental and calculated vibrational frequencies [cm^{-1}] of 1 .				
IR ^[a] (gas)	Raman (solid)	Raman (Ar matrix)	Calc. ^[b]	Assignment
3110 (vw)	3111(30) 3092(93)	3112(20) 3096(100)	3110 (1/74) 3103 (5/40)	$\nu(\text{C}-\text{H}^{\text{l}})$ $\nu(\text{C}-\text{H}^{\text{m}})$
1698(vs)	1675(73)	1681(43)	1664 (170/15)	$\nu(\text{C}=\text{C})$
1336(vs)	1323(17)	1321(15)	1303 (121/4)	$\nu_{\text{s}}(\text{CF}_3)$
1160(vs)	1160(18)	1168(26) 1132(15)	1152 (77/3) 1119 (283/2)	$\nu(\text{C}-\text{F}^{\text{l}})$ $\nu_{\text{as}}(\text{CF}_3)$
1106(vs)	1079 ^[c]	1082(22)	1068 (314/2)	$\nu_{\text{as}}(\text{CF}_3)$
883(w)	863(65)	867(37)	853 (21/5)	$\nu(\text{C}-\text{C})$

[a] Abbreviations for IR intensities: vs = very strong, s = strong, m = medium, w = weak. [b] Calculated on the PBE0/cc-pVTZ level of theory; Scaling factor 0.95; IR intensities in km mol^{-1} ; Raman intensities in $\text{\AA}^2/\text{u}$. [c] recalculated from the Fermi resonance doublet at 1098(15) and 1056(12) cm^{-1} .

displacement coordinates. For the *trans*-**1** with C_s symmetry 21 fundamentals (14 A' + 7 A'') are expected.

The C–H vibrations occur at 3112 [C(1)H] and 3096 cm^{-1} [C(2)H] in argon matrices and do not considerably differ from the frequencies observed in the solid state. The hydrogen atoms are involved in weak C–H...F hydrogen bonds in the solid phase and therefore a red-shift would be expected, but it should be kept in mind that guest-host interactions in matrices cause also a small red-shift.

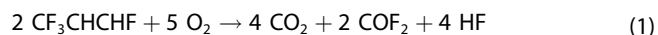
The C=C stretching vibration at 1681 cm^{-1} as well as the C–F stretching vibrations between 1132 and 1321 cm^{-1} are

observed in their typical regions. The C–C valence mode appears at 867 cm^{-1} which is quite a low frequency for carbon single bonds, but it is still in the expected region between 850 and 1150 cm^{-1} .^[29,30] This is surprising considering the short C–C bond (crystal 1.4789(3), gas 1.481(6) \AA , see above) and thus we attribute the low frequency to coupling effects. A similar observation was made for **2** with $\nu(\text{C}-\text{C})$ at 790 cm^{-1} ,^[7] whereas the bond lengths are more on the shorter range of C–C values (crystal 1.4963(4), gas 1.498(4) \AA , see above). The assignments of the deformation vibrations are listed in the Supporting Information (Table S9).

2.6. Combustion

For the **2** several combustion experiments as well as flammability, burning velocity and heat of combustion were determined.^[3,7,31–34] Far less is known about *trans*-**1** which is claimed to be not readily flammable, in contrast to the highly flammable **2**.^[35,36] Therefore we performed combustion experiments at different ratios of *trans*-**1** with oxygen and synthetic air. The combustion products were analyzed by infrared spectroscopy. Carbon dioxide, hydrogen fluoride and carbonyl fluoride were found as the main combustion products. As already reported for **2**, hydrogen fluoride was detected indirectly as SiF_4 ; this was formed by the reaction of HF with the glass wall of the reaction vessel. Carbon tetrafluoride was observed as a minor species.^[7]

With a sufficient amount of oxygen the combustion proceeds accordingly to Equation (1).



The combustion behavior is similar to that of **2**. Differences occur at sub-stoichiometric ratios of oxygen. The amount of COF_2 decreases, a part of *trans*-**1** remains unchanged, but considerable amounts of a black soot are formed. In general, the combustion of hydrofluorocarbons does not lead to the formation of considerable amounts of carbonyl fluoride. The hydrogen and fluorine atoms preferentially form the thermodynamically favored hydrogen fluoride during combustion. Consequently, the formation of COF_2 is only possible when the number of fluorine atoms is larger than that of hydrogen atoms in a molecule. But such molecules are usually non-flammable, thus formation of COF_2 has been only observed during pyrolysis on air.^[37] In this respect tetrafluoropropene **1** is an exception. The instability towards oxidation is based on the presence of the carbon–carbon double bond. This instability towards oxidants is also the reason for the short lifetime in the atmosphere and consequently its relatively low global warming potential of $\text{GWP}_{100} = 7$.^[11]

The classification of the flammability according to the European transportation standard ADR, which is worldwide used for transportation of dangerous goods, is based on the explosion region of a gas/air mixture. To the best of our knowledge the explosion region has been only determined by the ASHRAE method which has a different classification for

flammability.^[34–36] Therefore we determined the explosion (or flammability) region of *trans*-1 with air according to the European standard protocol EN 1839.^[38] The lower flammability limit (LFL) was found at 5.6% and the upper flammability limit (UFL) at 14.2%. These values are comparable with the ASHRAE method which yields values of LFL = 6.25% and UFL = 12.4%. In case of **2** the ASHRAE method yielded LFL = 6.82% and UFL = 12.0% whereas with the European standard setup values of LFL = 6.2% and UFL = 14.4% have been determined. The different values of both methods are probably caused by the differences in the experimental setups. The flammability region of *trans*-1 determined in our laboratories leads to a classification of a highly flammable gas. This finding together with the fact that highly toxic gases are formed in the case of fire should lead to a reconsideration of the safety risk assessments of *trans*-1.

3. Conclusions

The refrigerants *trans*-1,3,3,3-tetrafluoropropene (HFO-1234ze, **1**) and 2,3,3,3-tetrafluoropropene (HFO-1234yf, **2**) were investigated by high angle X-ray diffraction which allowed performing a topological analysis of their charge density distributions. Gas-phase electron diffraction yielded sets of structure parameters of the molecules free of intermolecular interactions. Vibrational spectra of *trans*-1,3,3,3-tetrafluoropropene (**1**) in all aggregation states and in matrices have been studied and the results were related to quantum-chemical values calculated at the PBE0/cc-pVTZ level of theory. Combustion experiments of *trans*-1,3,3,3-tetrafluoropropene (**1**) revealed carbon dioxide, carbonyl fluoride and hydrogen fluoride to be the main combustion products. The determination of the flammability region leads to the classification of *trans*-1,3,3,3-tetrafluoropropene (**1**) as a highly flammable gas.

Experimental Section

Materials

Samples (ca. 10 g) of *trans*-1,3,3,3-tetrafluoropropene (HFO-1234ze (E), Tyczka Industriegase, **1**) and 2,3,3,3-tetrafluoropropene (HFO-1234yf, Honeywell, **2**), respectively, were condensed into carbon-steel cylinders using a stainless-steel vacuum line. Residues of nitrogen were removed at -196°C in dynamic vacuum. The samples were checked for purity by GC-MS (Varian CP3800, mass spectrometer Saturn).

Crystals were measured on an Agilent SuperNova, Single Source at offset, Eos diffractometer using Mo-K α radiation ($\lambda = 0.71073 \text{ \AA}$) at 93.0(4) resp. 95.0(2) K. Using Olex2,^[39] the structures were solved with the ShelXT^[40] structure solution program using Dual Space and refined using XD-2006.^[41] All atoms were refined anisotropically. The data were corrected for absorption using SADABS.^[42] Plots about distribution of outliers, normal probability and fractal dimension in the SI were produced by WINGX.^[43]

Electron diffraction patterns for **1** and **2** were recorded on the heavily improved Balzers Eldigraph KD-G2 gas-phase electron diffractometer at Bielefeld University. Experimental details are listed

in Table S3 of the Supporting Information; instrumental details are reported elsewhere.^[44] The electron diffraction patterns, three for each, long and short nozzle-to-plate distances, were measured on Fuji BAS-IP MP 2025 imaging plates, which were scanned by using a calibrated Fuji BAS 1800II scanner. The intensity curves (Figures S1 and S2, Supporting Information) were obtained by applying the method described earlier.^[45] Electron wavelengths were refined^[46] using carbon tetrachloride diffraction patterns, recorded in the same series of experiments as the substances under investigation. Analysis of the measured electron diffraction intensities has been done using least-squares method. Geometrical models of the molecules have been defined in form of Z-matrices (see Supporting Information). Initial values of parameters and fixed differences between values of parameters in each group were taken from MP2/cc-pVTZ calculations. Amplitudes of interatomic vibrations and vibrational corrections have been calculated for both molecules with the VibModule program^[47] on the basis of harmonic and cubic force fields from PBE0/cc-pVTZ computations. For 2,3,3,3-tetrafluoropropene (**2**) a combined structure refinement was performed, using GED intensities and rotational constants, the relative weights for the latter were adjusted so that both GED *R*-factors and discrepancies in rotational constants were acceptable.

The Raman spectroscopic measurements were executed on a Bruker® MultiRAMII FT-Raman spectrometer equipped with a Nd:YAG laser ($\lambda = 1064 \text{ nm}$). The interpretation of the spectra was carried out with the aid of the software Advanced Chemistry Development, Inc.® (ACD/Labs 2015). Infrared spectra were recorded on a Bruker® Vertex-80 V-FT-IR spectrometer. The spectra were evaluated using the same software as for the Raman spectra. The matrix isolation apparatus and the general procedure for the preparation of matrix layers are described elsewhere.^[48] The matrix layers were prepared by condensation of 6 mmol premixed *trans*-1 and noble gas mixture at a continuous flow rate of 6 mmol h^{-1} ($130 \text{ cm}^3 \text{ h}^{-1}$) onto the cold tip at 10 K.

Combustion experiments were performed using the same apparatus and in the same manner as already reported for **2**.^[7] For the determination of the explosion region of *trans*-1 the protocol accordingly to the DIN EN 1839 standard was used (tube method).^[38] The experimental set-up shown in the Supporting Information (Figure S23) was calibrated with methane and synthetic air prior to use. For the experiments with *trans*-1 the synthetic air was moistened with distilled water as recommended for halogenated gases by the protocol. The explosion region of *trans*-1 was determined between 5.4% and 15.6%.

Acknowledgements

We gratefully acknowledge the financial support of the Deutsche Forschungsgemeinschaft (DFG), the Ludwig-Maximilians-Universität (LMU). We gratefully acknowledge computation time and QC programs provided by the RRZK (Universität zu Köln) and the PC² (Universität Paderborn). This work was funded by Deutsche Forschungsgemeinschaft DFG (German Research Foundation) through a core facility GED@BI grant MI477/35-1, project no. 324757882) and by a grant for YuVV (VI1713/1-2, project no. 243500032). Open access funding enabled and organized by Projekt DEAL.

Conflict of Interest

The authors declare no conflict of interest.

Keywords: refrigerants · high-angle X-ray diffraction · vibrational spectra · matrix isolation · combustion analysis

- [1] C. Hogue, *Chem. Eng. News* **2011**, 89, 31.
- [2] Ø. Hodnebrog, M. Etniman, J. S. Fuglested, G. Marston, G. Myhre, C. J. Nielsen, K. P. Shine, T. J. Wallington, *Rev. Geophys.* **2013**, 51, 300.
- [3] a) R. Akasaka *Int. J. Thermophys.* **2011**, 32, 1125; b) C. Di Nicola, G. Di Nicola, M. Pacetti, F. Polonara, G. Santori, *J. Chem. Eng. Data* **2010**, 55, 3302; c) G. Di Nicola, M. Moglie, *Int. J. Refrig.* **2011**, 34, 1098; d) L. Fedele, S. Bobbo, F. Groppo, J. S. Brown, C. Zilio, *J. Chem. Eng. Data* **2011**, 56, 2608; e) Y. Kano, Y. Kayukawa, K. Fujii, H. Sato, *Int. J. Thermophys.* **2010**, 31, 2051; f) S. Lago, P. A. G. Albo, S. Brignolo, *J. Chem. Eng. Data* **2011**, 56, 161; g) R. A. Perkins, M. L. Huber, *J. Chem. Eng. Data* **2011**, 56, 4868; h) M. Richter, M. O. McLinden, E. W. Lemmon, *J. Chem. Eng. Data* **2011**, 56, 3254; i) K. Tanaka, Y. Higashi, R. Akasaka, *J. Chem. Eng. Data* **2010**, 55, 901.
- [4] I. Skarmoutsos, P. A. Hunt, *J. Phys. Chem. B* **2010**, 114, 17120.
- [5] T. Soulestin, V. Ladmiraal, T. Lannuzel, F. D. D. Santos, B. Améduri, *Polym. Chem.* **2017**, 8, 735.
- [6] M. D. Marshall, H. O. Leung, B. Q. Scheetz, J. E. Thaler, J. S. Muentzer, *J. Mol. Spectrosc.* **2011**, 266, 37.
- [7] M. Feller, K. Lux, C. Hohenstein, A. Kornath, *Z. Naturforsch.* **2014**, 69b, 379.
- [8] a) J. P. Perdew, K. Burke, Y. Wang, *Phys. Rev. B* **1996**, 54, 16533; b) J. P. Perdew, K. Burke, M. Ernzerhof, *Phys. Rev. Lett.* **1997**, 78, 1396.
- [9] T. H. Dunning, *J. Chem. Phys.* **1989**, 90, 1007.
- [10] More details are listed in Table S2 of the Supporting Information. CCDC 1841624 (for 1) and 1841625 (for 2) contain the supplementary crystallographic data for this paper. These data can be obtained via www.ccdc.cam.ac.uk/data_request/cif free of charge from The Cambridge Crystallographic Data Centre.
- [11] P. Luger, A. Bach, J. Buschmann, D. Lentz, *Z. Kristallogr.* **2000**, 215, 518.
- [12] H. A. Bent, *Chem. Rev.* **1961**, 61, 275.
- [13] D. Lentz, A. Bach, J. Buschmann, P. Luger, M. Messerschmidt, *Chem. Eur. J.* **2004**, 10, 5059.
- [14] A. Bach, D. Lentz, P. Luger, M. Messerschmidt, C. Olesch, M. Patzschke, *Angew. Chem. Int. Ed.* **2002**, 41, 296.
- [15] D. Lentz, *J. Chem. Crystallogr.* **2003**, 33, 977.
- [16] S. Alvarez, *Dalton Trans.* **2013**, 42, 8617.
- [17] a) T. S. Koritsánszky, P. Coppens *Chem. Rev.* **2001**, 101, 1583; b) P. Coppens, *X-Ray Charge Densities and Chemical Bonding*, International Union of Crystallography, Chester, England, Oxford, New York, **1997**.
- [18] T. A. Keith, "AIMALL" (version 16.05.18), TK Gristmill Software Overland Parks KS, USA, can be found under aim.tkgristmill.com, **2016**.
- [19] a) R. F. W. Bader, *Atoms in Molecules. A Quantum Theory*, Clarendon Press, Oxford, **1994**; b) R. F. W. Bader *Chem. Rev.* **1991**, 91, 893.
- [20] a) P. Luger, J. Buschmann, T. S. Koritsánszky, D. Lentz, N. Nickelt, S. Willemsen, *Z. Kristallogr.* **2000**, 215, 487; b) D. Lentz, M. Patzschke, A. Bach, S. Scheins, P. Luger, *Org. Biomol. Chem.* **2003**, 1, 409; c) H.-G. Stammler, Yu. V. Vishnevskiy, C. Sicking, N. W. Mitzel, *CrystEngComm* **2013**, 15, 3536; d) J. Schwabedissen, P. C. Trapp, H.-G. Stammler, B. Neumann, J.-H. Lamm, Yu. V. Vishnevskiy, L. A. Körte, N. W. Mitzel, *Chem. Eur. J.* **2019**, 25, 7339.
- [21] Yu. V. Vishnevskiy, J. Schwabedissen, A. N. Rykov, V. V. Kuznetsoc, N. N. Makhova, *J. Phys. Chem. A*, **2015**, 119, 10871.
- [22] I. Tokue, T. Fukuyama, K. Kuchitsu, *J. Mol. Struct.* **1973**, 17, 207.
- [23] J. L. Carlos Jr., R. R. Karl Jr., S. H. Bauer, *J. Chem. Soc. Faraday Trans. 2* **1974**, 70, 177.
- [24] H. Bürger, G. Pawelke, H. Oberhammer, *J. Mol. Struct.* **1982**, 84, 49.
- [25] R. L. Hilderbrandt, A. L. Andreassen, S. H. Bauer, *J. Phys. Chem.* **1970**, 74, 1586.
- [26] I. L. Karle, J. Karle, *J. Chem. Phys.* **1950**, 18, 963.
- [27] F. C. Mijlhoff, G. H. Renes, K. Kohata, K. Oyanagi, K. Kuchitsu, *J. Mol. Struct.* **1977**, 39, 241.
- [28] A. H. Lowrey, C. George, P. D'Antonio, J. Karle, *J. Mol. Struct.* **1979**, 53, 189.
- [29] T. Soltner, N. R. Goetz, A. Kornath, *Eur. J. Inorg. Chem.* **2011**, 3076.
- [30] J. Weidlein, K. Dehnicke, U. Müller, *Schwingungsspektroskopie: eine Einführung*, Georg Thieme Verlag, Stuttgart, **1988**.
- [31] K. Takizawa, K. Tokuhashi, S. Kondo, *J. Hazard. Mater.* **2009**, 172, 1329.
- [32] B. H. Minor, D. Herrmann, R. Gravell, *Process Saf. Prog.* **2010**, 29, 150.
- [33] M. E. Koban, D. D. Herrmann, *Process Saf. Prog.* **2011**, 30, 27.
- [34] S. Kondo, K. Takahashi, K. Takizawa, K. Tokuhashi, *Fire Saf. J.* **2011**, 46, 289.
- [35] S. Kondo, K. Takizawa, K. Tokuhashi, *J. Fluorine Chem.* **2012**, 144, 130.
- [36] S. Kondo, K. Tokuhashi, K. Takizawa, *J. Fluorine Chem.* **2013**, 149, 18.
- [37] S. H. Modiano, K. L. McNesby, P. E. Marsh, W. Bolt, C. Herud, *Appl. Opt.*, **1996**, 35, 4004.
- [38] a) M. Krautwurst, *ADR*, 2nd Ed. **2019**, Verkehrsverlag J. Fischer GmbH und Co. KG, Düsseldorf; b) Deutsches Institut für Normung e.V. „Bestimmung der Explosionsgrenzen von Gasen und Dämpfen“ EN 1839:2012, **2014**, Beuth Verlag GmbH, Berlin.
- [39] O. V. Dolomanov, L. J. Bourhis, R. J. Gildea, J. A. K. Howard, H. Puschmann, *J. Appl. Crystallogr.* **2009**, 42, 339.
- [40] G. M. Sheldrick, *Acta Crystallogr. Sect. C* **2015**, 71, 3.
- [41] A. Volkov, P. Macchi, L. J. Farrugia, C. Gatti, P. R. Mallinson, Richter, T. Koritsánszky, **2006**, XD2006.
- [42] Sadabs, **2012/1**, Bruker AXS Inc., Madison, Wisconsin, USA.
- [43] L. J. Farrugia, *J. Appl. Crystallogr.* **2012**, 45, 849.
- [44] a) R. J. F. Berger, M. Hoffmann, S. A. Hayes, N. W. Mitzel, *Z. Naturforsch.* **2009**, 64b, 1259; b) C. G. Reuter, Yu. V. Vishnevskiy, S. Blomeyer, N. W. Mitzel, *Z. Naturforsch.* **2016**, 71b, 1.
- [45] Yu. V. Vishnevskiy, *J. Mol. Struct.* **2007**, 833, 30.
- [46] Yu. V. Vishnevskiy, *J. Mol. Struct.* **2007**, 871, 24.
- [47] Yu. V. Vishnevskiy, Yu. A. Zhabanov, *J. Phys. Conf. Ser.* **2015**, 633, 012076.
- [48] A. Kornath, *J. Raman Spectrosc.* **1997**, 28, 9.

Manuscript received: June 8, 2020

Revised manuscript received: July 20, 2020